 DOI: 10.1002/masy.200750905

Spectroelectrochemical Reactivities of Novel Polyaniline Nanotube Pesticide Biosensors

*V. Somerset, M. Klink, R. Akinyeye, I. Michira, M. Sekota, A. Al-Ahmed, P. Baker, E. Iwuoha**

Summary: The preparation and characterisation of electrosynthetic polyaniline nanomaterials doped with phenanthrene sulphonic acid (PSA) is being presented. The polymeric nanomaterials prepared include processable poly(*o*-methoxy aniline) (POMA) and poly(2,5-dimethoxy aniline) (PDMA). Spectroelectrochemical reactivities of the electroactive polymeric nanotube systems as well as the nanobiosensor systems were studied by SEM, FTIR, UV-Vis and Subtractively Normalised Fourier Transformed Infrared Spectroscopy (SNIFTIRS) techniques. Furthermore, cyclic and differential pulse voltammetric studies of the nanomaterials were also performed using platinum or thiol-modulated gold electrodes. The SEM studies confirmed the nanorod morphology of the polyanilines. The heterogeneous rate constant, k_o, for the nanopolymeric material and the diffusion coefficient of electrons, D_e, was calculated and found to be in agreement with values expected for electron hopping along conducting polymer chains. Organophosphate pesticide nanobiosensor devices were prepared by encapsulating acetylcholinesterase (AChE) in the nanopolymeric composite. The biosensor amperometric response to the organophosphate pesticide called diazinon and the carbamate pesticide called carbofuran were studied. The sensor responses to pesticides followed typical electrochemical Michaelis-Menten kinetics.

Keywords: biosensor; nanotube; pesticide; polyaniline; Spectroelectrochemistry

Introduction

One conducting polymer that has received greater attention is polyaniline (PANI), due to its ease of preparation and well behaved electrochemistry. On the other hand, PANI has low solubility in common organic solvents and thus an ultimate restricted processability. Improving the solubility of PANI in organic solvents has been the focus of several studies, to enable its utilisation for suitable applications. The use of functional acids serving as dopants has been used as methods to improve the solubility of PANI.[1–3]

Recent studies[4–8] have shown that polyaniline nanoparticles (nanoPANI) can be developed with relative ease in aid to overcome some processability issues associated with PANI. Morrin et al.[4] have shown that the nanoPANI exhibit unique properties such as greater conductivity and more rapid electrochemical switching speed. Furthermore, the nanoPANI is said to offer bulk solution handling characteristics with nanoscale material control, while it offers combination with enzymes for biosensor construction.

The increasing interest in the use of polyanilines (PANIs) as conjugated polymers stems from its uniqueness among other conjugated polymers, because its properties can be reversibly controlled by both redox doping and protonation.[9] The use of functional acids serving as dopants has been used as methods to improve the

Sensor Research Laboratory, Department of Chemistry, University of the Western Cape, Bellville, 7535, South Africa
E-mail: eiwuoha@uwc.ac.za

solubility of PANIs. The dopants that are commonly known include *p*-toluene-sulphonic acid (TSA), dodecyl benzene-sulphonic acid (DBSA) and camphor-sulphonic acid (CSA). Another method that results in a more soluble conducting polymer is the polymerisation of a typical derivative of aniline, e.g. *2*-methoxyaniline (*o*-anisidine) or *2,5*-dimethoxyaniline. The substituent groups present in the units of PANI polymer chain causes a decrease in the stiffness of the polymer chain resulting in better solubility.

The poly(*o*-methoxyaniline) (POMA) molecule consists of two segments, i.e. a flat structure of two imine groups and a quinoid ring, as well as tetrahedral segments of two amine groups separating three benzoid rings as shown in Scheme 1. The presence of the aromatic rings in the POMA chain makes the polymer rigid and it mostly turn into an expanded coil conformation. The coil formation is enabled by the separation of each two aromatic rings with a nitrogen atom. Their repulsion should cause straightening of the chain, which is extremely beneficial for delocalisation of the electrons (charges) along the chain, and the formation of the energetically, most favourable polaronic structure. This however, is not a simple process. The polymer conformation can be strongly influenced by a dopant, as well as a solvent during the preparation process. For instance, if the anions of the dopant for the reason of their bulkiness cannot quickly diffuse in between the chains following the delocalising positive charges, one can expect that the chain expansion will be hindered.[10]

Redox activity of POMA enables variations in the relationship between the reduced amine and the oxidised imine groups in the polymer backbone, as shown in Scheme 1.

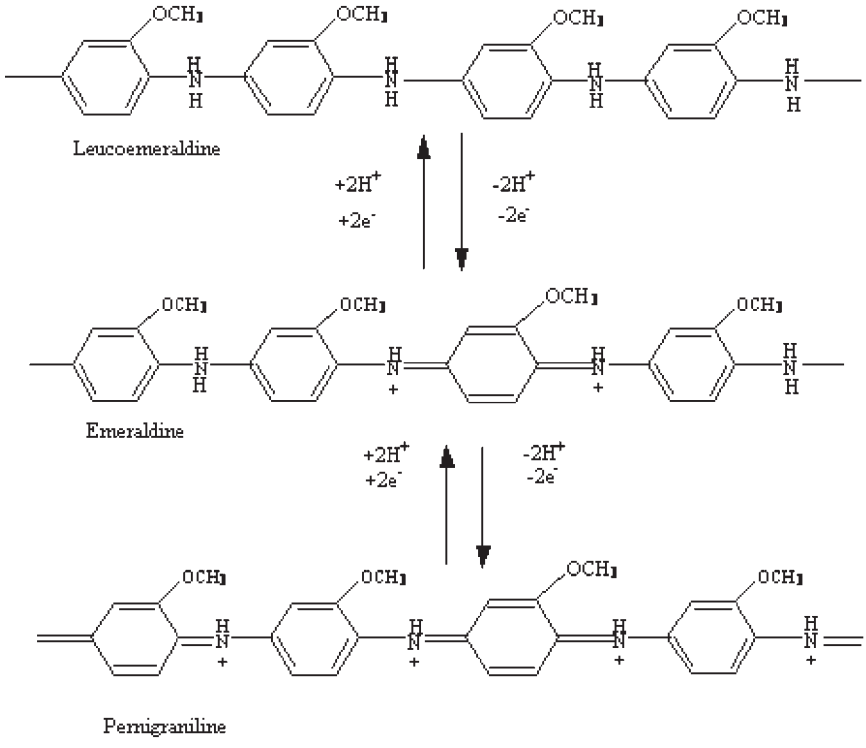

Scheme 1.
Schematic diagram of the molecular structures of leucoemeraldine, emeraldine and pernigraniline bases of poly(*o*-methoxyaniline) (POMA).

Scheme 1 further shows that the reduced amine and oxidised imine groups of POMA results in the polymer being in three possible oxidation states, namely leucoemeraldine base (LB), emeraldine base (EB) and pernigraniline base (PB). PANI systems are also of interest due to their ability to conduct electricity and related electrical properties. The use of protonic doping can result in a conductivity increase of the material by more than 10 orders of magnitude, from a non-conducting regime to good insulators to nearly metallic conductivity.[9]

If the EB form of POMA is subjected to protonic acid doping, it results in the formation of a polyelectrolyte, i.e. the polymer bearing a number of ionisable groups. The polyelectrolyte molecule can also be considered as an ideal molecular wire possessing metallic properties. Although the protonic acid doping is simple, it is not the only way of obtaining the EB based polyelectrolyte. Other few direct factors include redox-active agents, ionic salts, environmental conditions such as solvate medium, which lead to the formation of the emeraldine based polyelectrolyte chains with specific properties. Furthermore, the properties of the polyelectrolyte in a solid state are additionally affected by chain-chain interactions and therefore are sensitive to local ordering (packing) of the chains.[9]

The focus of the research in this study was to employ polyaniline as a mediator in the construction of a biosensor for pesticide detection. Pesticides such as carbamates and organophosphates represent a potential hazard to the environment and human health, since they not only inhibit insect acetylcholinesterase (AChE), but they also strongly interfere with neural transmissions in humans. These pesticides therefore need continuous assessment and monitoring. What are also needed are sensitive, rapid and reliable methods for the determination of these compounds in environmental samples in order to protect the environment and human health. The analysis of pesticides is currently based on methods using complex laboratory-based instrumental techniques such as high-performance liquid chromatography (HPLC) and gas chromatography (GC). Although these methods have very good sensitivity and reliability, they cannot be carried out in the field (rivers, lakes, etc.). They are also time-consuming and require expensive instrumentation and have to be operated by highly trained personnel.[11,12]

Biosensors can be constructed to be effective measurement tools for pesticides, since they are potentially small, robust, portable and easy to use, capable of providing reliable analytical information in a continuous fashion. However, it should be mentioned that they aim of the biosensor constructed in this paper, is not to compete with the proven powerful techniques of HPLC and GC. The objective is rather to develop a biosensor that can be applied to provide quick and reliable information on pollutants from real samples in the field. Since in the field the analyte is present in a complex matrix and can then be detected when its concentration is higher than the detection limit of the device.[13]

The aim of our research was to first use a new dopant called phenanthrene sulphonic acid in the chemical synthesis of the novel nanoPANI materials. The structure and morphology of the nanomaterials were elucidated using techniques such as scanning electron microscopy (SEM), electrochemical voltammetric analysis, UV-Vis absorption and molecular vibrational spectroscopy (FTIR). Secondly the aim of this study was to develop a simple and sensitive amperometric method for direct measurement of organophosphate and carbamate pesticides, which will later be applied to the determination of these pesticides in organic solvents. Existing enzyme sensors described for the detection of organophosphates and pesticides are based on the anodic oxidation of thiocholine obtained by the hydrolysis of butyryl- or acetylthiocholine or the acetylcholine substrates. Our strategy is based on using the following signal amplifying systems: (i) applying a self-assembling monolayer (SAM) of mercaptobenzothiazole (MBT)

to the gold electrode surface for pre-organisation of the polymer film; drop coating of the nanoPANI materials on the Au/MBT electrode; (iii) immobilisation of the enzyme AChE in the polymeric composite. One of the determinant factors in the development of a fast and sensitive AChE-sensor is the method employed for the enzyme immobilisation to the electrode surface. This was the rationale behind the coating of the thiol MBT to the electrode surface, which in turn place a role in the re-organisation of the nanoPANI polymer composite for easy cross-linking and immobilisation of the enzyme.

Experimental Part

Materials and Reagents

Reagents *o*-anisidine (99%), *2,5*-dimethoxyaniline (99%), potassium dihydrogen phosphate (99+%), disodium hydrogen phosphate (98+%), phenanthrene (99%) and potassium bromide (99+%) were obtained from Aldrich, Germany. Fluka (Germany) supplied the mercaptobenzothiazole (MBT), acetylcholinesterase (AChE, from Electrophorus electricus, EC 3.1.1.7), acetylthiocholine chloride (99%), sodium hydroxide (99%), dimethyl sulfoxide (99.6+%), ammonium persulfate (98%), methanol (99.8%) and dimethyl ether (99.9%). Merck's potassium chloride, sulphuric acid (95%), hydrochloric acid (32%) and ethanol (absolute, 99.9%) were used in the experiments. The organic solvents ethanol (pestanal grade, 99.9%) and acetone (pestanal grade, 99.8%) were purchased from Riedel-de Haën, Germany. All electrochemical measurements were carried out in phosphate buffered saline (PBS) solution (0.1 M phosphate, 0.1 M KCl, pH 7.2).

Apparatus

All electrochemical measurements were performed using a BAS 50 W potentiostat {Bioanalytical Systems (BAS), Lafayette, IN, USA} using cyclic voltammetry (CV), Osteryoung square wave voltammetry (OSWV) and differential pulse voltammetry (DPV) amperometric modes. A conventional three electrode system was employed: BAS 1.6 mm diameter Au (or Pt) disc working electrode, BAS 3 M NaCl-type Ag/AgCl reference electrode and a platinum wire auxiliary electrode. A convectional (10 ml) one compartment and three electrode configuration cell was employed. Prior to use the working electrode was polished on aqueous slurries of 1.0, 0.3 and 0.05 μm alumina pads (Buehler) to give a final mirror finish. All aqueous solutions were freshly prepared by use of Millipore milli QTM water.

Synthesis of polyaniline(PANI)-phenanthrene Sulphonic Acid Nanomaterials

The synthesis of the phenanthrene sulphonic acid was done according to the following procedure. A solution containing 10 ml of fuming H_2SO_4 was diluted with 10 ml of 6 M H_2SO_4 and the mixture was diluted with water to 100 ml in a volumetric flask. 50 ml of the above solution was added to a round bottom flask that contained 2 g of phenanthrene. The contents were heated to boiling in an oil bath (temperature between 100–140 °C) fitted with a condenser and thermometer. The mixture was refluxed for 3 hrs with constant stirring to immerse reactants into solution. The mixture was then poured into crushed ice for 20 minutes and the unreacted phenanthrene was filtered off. 10 ml of a 50% 3 M NaOH solution was added to the mixture and put in a refrigerator to crystallise, to form a white phenanthrene sulphonic salt. The salt was then hydrolysed to form the phenantrene sulphonic acid.

This was followed by using *2,5*-dimethoxyaniline (0.0334 g), 20 ml of deionized water and phenanthrene sulphonic acid (PSA) (0.2592 ml) and placing it in a 100 ml beaker. The mixture was heated for 30 min at 50 °C while stirring vigorously. An aqueous solution of ammonium persulphate (APS) (0.1 M) was added dropwise to the hot solution. The mixture was cooled down to room temperature while continuously

stirring for 15 hours. The product was filtered and washed with deionised water, methanol and dimethyl ether 3 times respectively, to remove impurities such as APS, free PSA and unreacted *2,5*-dimethoxyaniline. The same procedure was used for the synthesis of poly(*o*-methoxyaniline)-phenanthrene sulphonic acid nanomaterials, except that 0.26 ml of *o*-methoxyaniline (*o*-anisidine) was used in stead of *2,5*-dimethoxyaniline.

Spectroelectrochemical Characterisation of polyaniline(PANI)-phenanthrene Sulphonic Acid Nanomaterials

The UV-Vis absorbance experiments were performed with UV-Vis 920 Spectrometer (GBC Scientific Instruments, Australia). Samples for UV-Vis analysis were first electrodeposited on the platinum working electrode through an anodic oxidative process. The polymer modified electrodes were placed in 5 ml dimethylsulfoxide (DMSO) solution and the resultant green solutions scanned in an experimental wavelength range between 200–900 nm.

For FTIR characterisation, the samples for the IR measurements were electrodeposited on a Pt working electrode employing 40 cycles of potential cycling at a scan rate of 100 mV/s. The potential was scanned between −400 and +800 mV potential limits for the nanoPOMA and nanoPDMA materials. The resultant polymer electrodes were rinsed in distilled water and dried under a dynamic vacuum for ca. 1 hr before scrapping on to 0.4 g of oven dried KBr (80 °C) followed by thorough grinding in a mortar to a slight greenish colouration. The polymer-KBr pellets were scanned on a Perkin Elmer Paragon 1000 PC FTIR, in the range 400–4000 cm^{-1} wave numbers.

Subtractively Normalised Fourier Transformed Infrared Spectroscopy (SNIFTIRS) data was collected as follows. The acquisition of interferograms was done at two different potentials E_i and E_f. The spectra were calculated as the relative reflectivity change $\Delta R/R = (R_{Ei} - R_{Ef})/R_{Ei}$. The potential was scanned between −200 and +500 mV vs. Ag/AgCl.[14]

Preparation of AChE Biosensor on Au/MBT/POMA-PSA Polymer Film

Prior to use, a gold disc electrode was first etched for about 5 min in a hot 'Piranha' solution {1:3 (v/v) 30% H_2O_2 and concentrated H_2SO_4}. It was then polished on aqueous slurries of 1, 0.3 and 0.05 μm alumina powder. After thorough rinsing with deionised water followed by acetone, the electrodes were cleaned electrochemically by cycling it between −200 and 1500 mV in 0.05 M H_2SO_4 at a scan rate of 10 mV/s for 10 min or until the CV characteristics for a clean Au electrode were obtained. The self-assembled monolayer (SAM) of mercaptobenzothiazole (MBT) was formed by immersing the cleaned Au electrode into an ethanolic solution of 10 mM of MBT for 2 hours. The Au/MBT SAM electrode was rinsed with copious amount of ethanol and water and stored in 0.1 M phosphate buffer (pH 7 = 7.2) solution for later use.

For the construction of the biosensor, the nanoPOMA-PSA was drop coated on the gold-MBT electrode using a freshly prepared 5 ml solution of 2.4 g of nanoPOMA-PSA in distilled water and allowing it to dry. This was followed by reducing the film in a 0.1 M phosphate buffer solution, pH 7.2 at −500 mV for approximately 25 min. Oxidation of the film followed in the presence of 60 $\mu g.ml^{-1}$ AChE at +400 mV vs. Ag/AgCl for 1500 s, sample interval of 500 ms and a sensitivity of 1×10^{-6} $A.V^{-1}$ and duration of approximately 30 min. During this oxidation process the enzyme becomes electrostatically attached to the Au/MBT/POMA-PSA polymer surface to give an electrode profile represented by Au/MBT/POMA-PSA/AChE.

Inhibition Plots for Organophosphate and Carbamate Pesticide Detection

Inhibition plots for each of the organophosphorous and carabamate pesticides detected were obtained using the percentage inhibition method. The following procedure was used. The biosensor was first placed in a stirred 0.1 M phosphate buffer, 0.1 M KCl (pH 7.2) solution (anaerobic conditions) and multiple additions of a standard AChCl substrate solution was

added until a stable current was obtained. This steady state current is related to the activity of the enzyme in the biosensor when no inhibitor is present. This was followed by thoroughly cleaning the biosensor with the working buffer solution, followed by incubating the biosensor in anaerobic conditions for 20 min with a standard pesticide plus 0.1 M phosphate, KCl (pH = 7.2) buffer-organic solvent mixture. Then multiple additions of a standard AChCl substrate solution was again added until a stable current was obtained. The percentage inhibition was then calculated using the formula:

$$I\% = \frac{(I_1 - I_2)}{I_1} \times 100$$

where I% is the degree of inhibition, I_1 is the steady-state current obtained in buffer solution, I_2 is the steady-state current obtained after the biosensor was incubated for 20 min in phosphate buffer-organic solvent mixture.[15–17]

Results and Discussion

Scanning Electron Microscopy (SEM) Results of nanoPANI Materials

Scanning electron microscopy studies were performed on the nanoPANI materials and the results are shown in Figure 1 and 2. The aim of the SEM studies was to investigate whether the dopant phenanthrene sulphonic acid (PSA) was able to affect the polymerisation synthesis of the polymers PDMA and POMA, and what molar doping ratio should be used in order to have polymers with nanodimensions in its morphology and structure.

In Figure 1 the morphology and structure of the polymer, PDMA with the dopant PSA is shown.

The results in Figure 1 shows that when the molar doping level of PDMA:PSA was decreased from 1:2 down to 1:0.5, clusters of nanorods were observed in the morphology and structure of the nanomaterials. Furthermore, these nanorods have a diameter of approximately 200 nm as can be seen in the SEM micrograph of Figure 1.

In Figure 2 the SEM micrograph of POMA doped with PSA can be seen. Similarly, it was found that a doping ratio of POMA:PSA = 1:0.5, showed nanorod clusters that formed when POMA is used as polymer in the synthesis of nanomaterials. The nanorods have an approximate diameter of 200 nm as can be seen in the SEM micrograph of Figure 2.[18]

Cyclic Voltammetric Characterisation of nanoPANI Materials

After synthesis of the nanoPANI materials, cyclic voltammetric studies were performed on the materials to investigate whether the

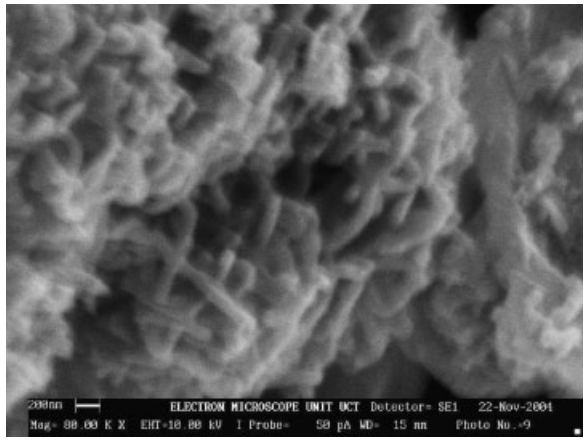

Figure 1.
SEM micrograph of PDMA-PSA nanorod clusters.

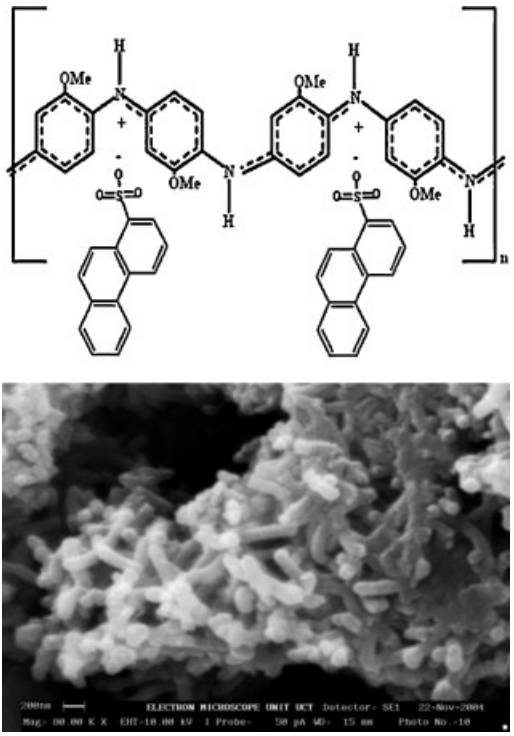

Figure 2.
SEM micrograph of POMA-PSA nanorod clusters and a chemical diagram representing the incorporation of PSA into the PANI backbone.

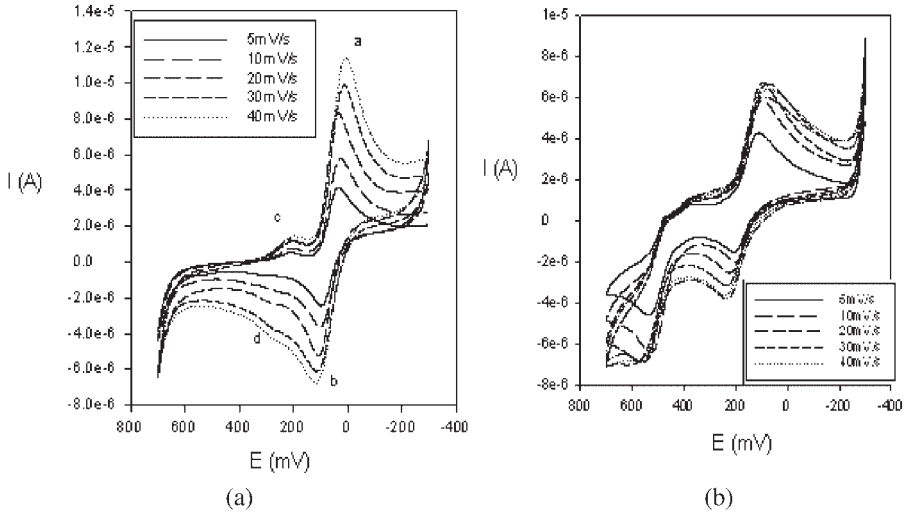

Figure 3.
Cyclic voltammograms for nanoPDMA-PSA material in (a) and nanoPOMA-PSA material in (b), scanned in the potential window between −400 and +800 mV (vs. Ag/AgCl) in 1M HCl at 25 °C, and at scan rates of 5, 10, 15, 30, 40 and 50 mV/s.

oxidation and reduction peaks of PANI can be seen.

Figure 3(a) shows the cyclic voltammogram (CV) of the nanoPOMA-PSA material on a Pt electrode in 1 M HCl solution with increasing scan rates of 5, 10, 15, 30, 40 and 50 mV/s. The CV shows that the peak potentials and peak currents are increasing as the scan rate is increased. This is indicative of a conducting polymer and it further shows that diffusion of electrons takes place along the polymer chain. Strong redox peaks are seen in (b) at +101.7 mV vs. Ag/AgCl and in (a) at 46.0 mV vs. Ag/AgCl. The oxidation peak in (b) shows the polymer being transformed from the leucoemeraldine base (LB) to the emeraldine salt (ES) and peak (d) shows ES transformed to the pernigraniline salt (PS) of PANI. On the reverse scan the nanoPANI is transformed from PS to ES in peak (c) and from ES to LB in peak (a).

In Figure 3(b) the cyclic voltammogram (CV) of nanoPDMA-PSA material on a Pt electrode in 1 M HCl solution with increasing scan rates at 5, 10, 15, 30, 40 and 50 mV/s are shown. Analysis of the voltammograms shows that the peak potentials and corresponding currents vary at the different scan rates. This is an indication that the polymer nanorods are electroactive and the electron transfer processes are coupled to a diffusion process namely, charge transportation along the polymeric nanorods. Furthermore, 2 anodic and 3 cathodic peaks were observed. The first oxidation peak at +172.1 mV vs. Ag/AgCl shows the nanoPANI transformed from the leucoemeraldine base (LB) to the emeraldine salt (ES) and ES to pernigraniline salt (PS) at a potential of +577.0 mV vs. Ag/AgCl. On the reverse scan, the peaks correspond to the conversion of PS to ES and ES to LB, respectively. The small reduction peak on the reverse scan is associated with the formation of hydroquinone as a side product of PANI upon cycling the potential.[4,19–21]

The nanoPANI materials were further subjected to Randel-Sevcik analysis[22] for the determination of the electron diffusion coefficient (D_e) and the results were found to be in agreement with the values obtained for the electrosynthesis of PANI.[20,21] D_e gives an indication of the rate of charge transfer along the polymer chain. In case of the nanoPDMA materials, the value of D_e was estimated to be 2.01×10^{-9} $cm^2 \cdot s^{-1}$, while a D_e value of 8.68×10^{-9} $cm^2 \cdot s^{-1}$ was obtained for the electrosynthesised PANI[21] and 6.46×10^{-8} $cm^2 \cdot s^{-1}$ for electrosynthesised PANI-Polyvinyl sulphonate.[20] Furthermore, the heterogeneous rate constant (k_0) for the nanoPANI materials was also calculated and found to be 5.59×10^{-5} $cm \cdot s^{-1}$ for PDMA- PSA and 8.89×10^{-7} $cm \cdot s^{-1}$ for POMA-PSA.

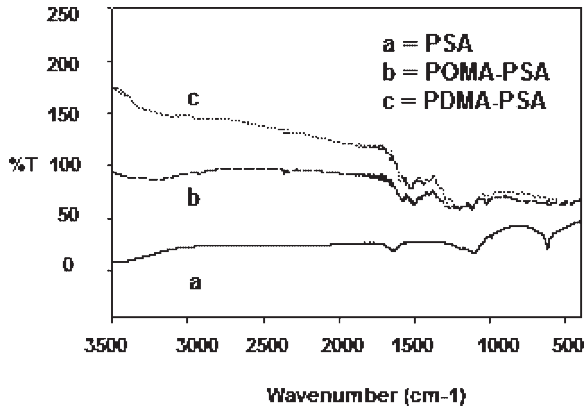

Figure 4.
FTIR spectra of the nano POMA-PSA and PDMA-PSA materials.

FTIR Spectroscopic Characterisation of nanoPANI Materials

The structural characteristics of the nanoPANI materials were secondly investigated using FTIR spectroscopy in the range 3500 to 500 cm^{-1} and the results are shown in Figure 4.

Absorption bands between 3500 and 3000 cm^{-1} (although weak) relate to the stretching of N–H bonds in the PANI backbone of the nanorods. The absorbance values at 1590 and 1520 cm^{-1} are due to the stretching vibrations in quinoid and benzoid rings respectively in the different polymers and characteristic of PANI.[18]. The bands at 1115, 1023 and 790 cm^{-1} are revealed to the 1–4 substitution on the benzene ring in PDMA. The band at 1174 cm^{-1} is considered as a measure of the degree of delocalisation of electrons on PDMA. The absorption band around 900 cm^{-1} attributes the 1–2 substitution on the benzene ring in POMA. 3 distinct bands were seen for PSA at 600, 1100 and 1800 cm^{-1}. These bands can be seen in the PDMA-PSA and POMA-PSA spectrum, which confirms the incorporation of PSA into the polymer backbone.[23,24]

UV-Vis Absorption Spectra of nanoPANI Materials

Figure 5 shows the UV-visible spectra of the phenanthrene sulphonic acid doped poly(*2,5*-dimethoxyaniline) (PDMA) and poly(*o*-methoxyaniline) (POMA) polymers in dimethyl sulphoxide (DMSO) as solvent. The UV-Vis results for the nanoPDMA-PSA and nanoPOMA-PSA in Figure 5 are of primary interest but are shown with that of PDMA doped with anthracene sulphonic acid (ASA) and HCl respectively in DMSO solution. The UV-vis absorption spectra of the nanoPDMA-PSA and nanoPOMA-PSA are shown with the dotted lines on the graphs. The UV-Vis results for the nanoPDMA-PSA materials shows 3 absorption bands at the wavelengths 350, 600 and 800 nm respectively. In the case of the nanoPOMA-PSA materials only 2 absorption bands around 350 and 600 nm can be seen. The 350 nm band is often assigned to the π-π^* transition in the benzoid structure of PANI, while the absorption in the visible range at 600 nm can be ascribed to exciton formation in the quinoid rings of PANI.[25] The band around 800 nm (bipolaron) can be associated to the charge carriers in the polymer chain.[26–28]

SNIFTIRS Spectroelectrochemistry Results of nanoPANI Materials

Subtractively Normalised Fourier Transformed Infrared Spectroscopy (SNIFTIRS) results were also recorded for the nanoPANI materials. The general shape of the spectra obtained in the SNIFTIRS method is displayed in Figure 6 and 7.

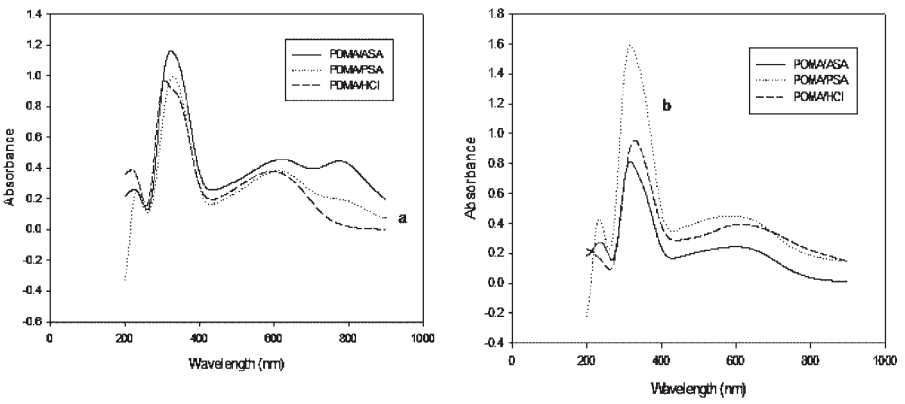

Figure 5.
UV-visible absorption spectra of the nanoPDMA-PSA materials in (a) and nanoPOMA-PSA materials in (b).

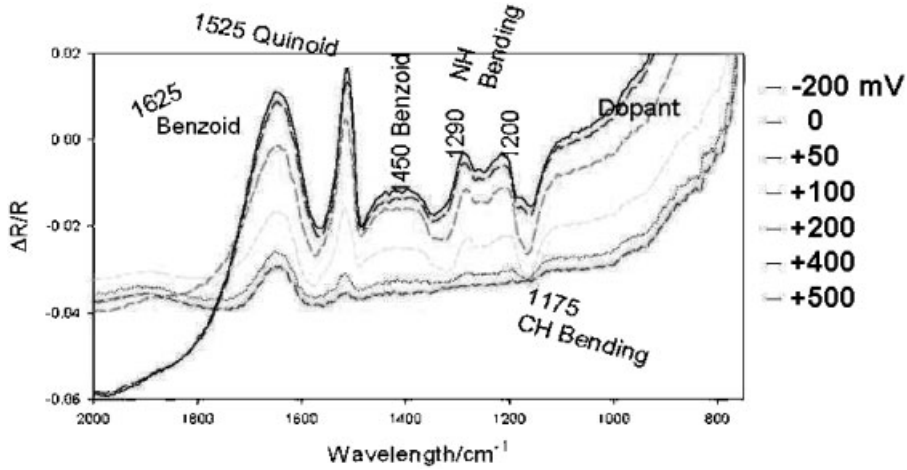

Figure 6.
SNIFTIRS spectra recorded for the Pt/nanoPDMA-PSA material.

For the nanoPDMA-PSA material in Figure 6, peaks were observed at 1625, 1525 and 1450 cm^{-1} and are due to the C=C vibrations of the quinoid benzoid rings. The peaks at 1290 and 1200 cm^{-1} can be assigned to the vibrations emanating from the N–H bond, while the peak at 1175 cm^{-1} is that of the C–H bending in the benzoid ring. Very small peaks at approximately 100 cm^{-1} were seen for the PSA dopant incorporated in the PDMA structure.[14,29]

The results for the nanoPOMA-PSA material in Figure 7 shows peaks at 1595, 1265 and 1232 cm^{-1} that are also due to the C=C vibrations of the quinoid benzoid rings. The peaks at 1295, 1265 and 1232 cm^{-1} are due to the N–H bond vibrations and the peak at 1150 cm^{-1} can again be assigned to the C–H bending in the benzoid ring. A more defined peak at 1050 cm^{-1} can be seen for the PSA dopant incorporated in the POMA structure.[14,29]. These results in Figure 6 and 7 for the different substituted PANIs are very similar and clearly elucidate the structure of the nanoPANI materials that were synthesized.

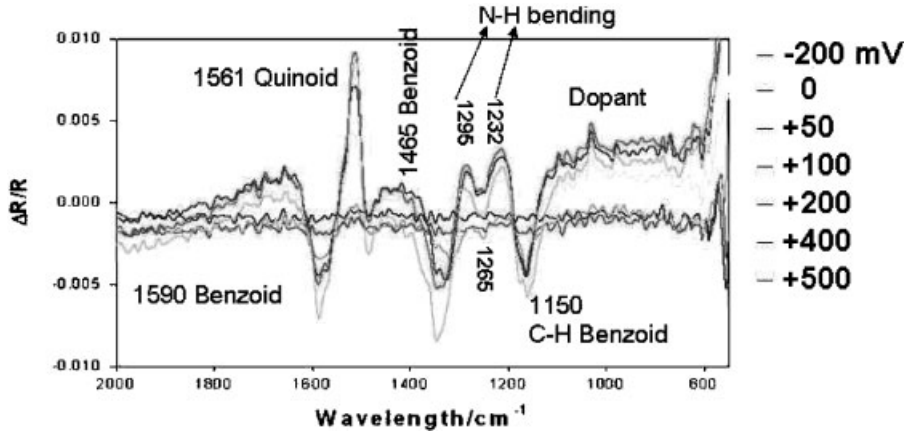

Figure 7.
SNIFTIRS spectra recorded for the Pt/nanoPOMA-PSA material.

Voltammetric Responses for Au/MBT/POMA-PSA/AChE/ACh Biosensor

The formation of self-assembled monolayers (SAMs) of organosulphur compounds on gold electrodes are of current research interest since the organosulphur compounds offer well organised, stable and compact self-assembled monolayers. SAM modified electrodes are used in the construction of electrochemical biosensors for the following reasons: (i) they can enhance the selectivity and sensitivity, (ii) improve the response time, (iii) decrease the overpotential, (iv) ease of preparation, (v) stability, and (vi) the possibility to introduce different chemical functionalities.[1,30–33]

Thiol monolayers form a group of chemical compounds that can be used to influence the properties or topological structure of chemically or electrochemically synthesized conducting polymers. Thiols can be applied to pre-organise monomers in one plane to allow subsequent polymerisation. This can be achieved by covalent or ionic immobilisation of monomer molecules and their electrochemical oxidation, leading to the formation of monomolecular films of conducting polymers on the surface.[30] The formation of a monolayer of mercaptobenzothiazole (MBT) was chosen, since it contains an aromatic ring with a fused thiazole ring, instead of a long alkyl chain.

The constructed sensor was then applied to detect the organophosphate and carbamate pesticides called diazinon and carbofuran respectively, based on the inhibition of the enzyme AChE by these pesticides.[15–17]

In Figure 8 below the anodic difference square wave voltammetry (SWV) results for the successive Diazinon pesticide addition to the Au/MBT/POMA-PSA/AChE/ACh biosensor in 0.1 M phosphate buffer, KCl (pH 7.2) is shown.

The results display the addition of 1.1 mM of ACh substrate in (a), while a shift in anodic current is observed after the addition of Diazinon pesticide concentrations of 0.18 ppb in (b) to 1.19 ppb in (g). This shift in anodic current shown in the SWV results can be attributed to the inhibition of the AChE enzyme by the diazinon pesticide.

When inhibitors such as the organophosphorous pesticides are present in a solution matrix, they inhibit some of the active centres of the AChE enzyme, producing an electroactive product that diminishes and

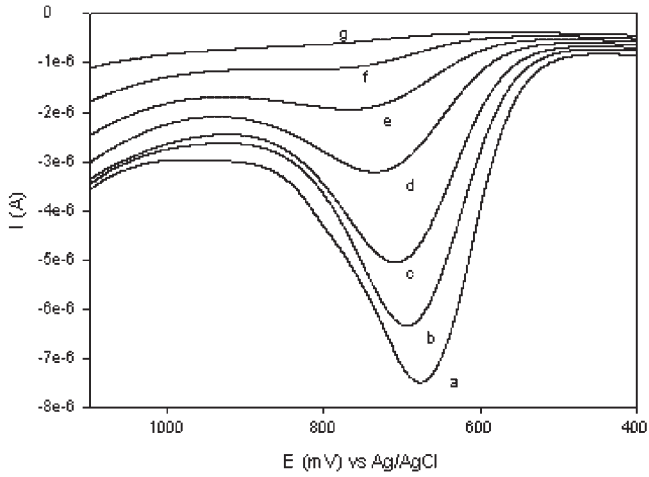

Figure 8.
The SWV responses for the successive diazinon pesticide additions to the Au/MBT/POMA-PSA/AChE/ACh biosensor in 0.1 M phosphate buffer, KCl (pH 7.2), with the potential scanned between +400 to +1100 mV at a frequency of 5 Hz, is shown.

signal decreases are shown. The decrease observed is related to the concentration of the pesticide in an amperometric sensor. It should also be noted that one of the major limitations in the detection of organophosphorous and carbamate pesticides, is the irreversible inhibition of the enzyme in the biosensor, disabling the reuse of the devices. This limitation can be circumvented with single-use biosensors.[33].

The square wave voltammetric (SWV) results in Figure 8 were further used to calculate the percentage inhibition of the Au/MBT/POMA-PSA/AChE/ACh biosensor by diazinon, using the formula:

$$I\% = \frac{(I_1 - I_2)}{I_1} \times 100$$

where $I\%$ is the degree of inhibition, I_1 is the current obtained after the addition of ACh substrate, and I_2 is the current obtained after Diazinon pesticide addition to the biosensor.[16–17,34]

Further analysis of the results in Figure 8 was done and in calculating the percentage inhibition it was found that when the enzyme AChE was exposed to diazinon concentrations of 1.19 ppb, substantial inhibition of 91% for the enzyme was observed.

Similarly as in Figure 8, the differential pulse voltammetric (DPV) responses (not shown here) were measured for the interaction of the Au/MBT/POMA-PSA/AChE/ACh biosensor in 0.1 M phosphate buffer, KCl (pH 7.2), with carbofuran as pesticide. For this biosensor analysis it was found that when the biosensor was exposed to a carbofuran concentration of 1.19 ppb, the percentage inhibition was less at 45%.

In the next step a plot of percentage inhibition versus – log pesticide concentration was constructed as shown in Figure 9 for carbofuran as pesticide. From the analysis of the inhibition plot for this biosensor the corresponding theoretical detection limit was determined for each of diazinon and carbofuran as pesticide on different plots. For the results in Figure 9 a sensitivity of - 33.20 (%I/decade) was determined from the slope of the graph and r^2 equal to 0.9590 was obtained with standard deviations of 3%.

From the percentage inhibition plots for diazinon (not shown here) and carbofuran (Figure 7) it was determined that the theoretical detection limit of the Au/MBT/POMA-PSA/AChE/ACh biosensor to diazinon as pesticide is 0.14 ppb. For carbofuran the theoretical detection limit was found to be 0.06 ppb.

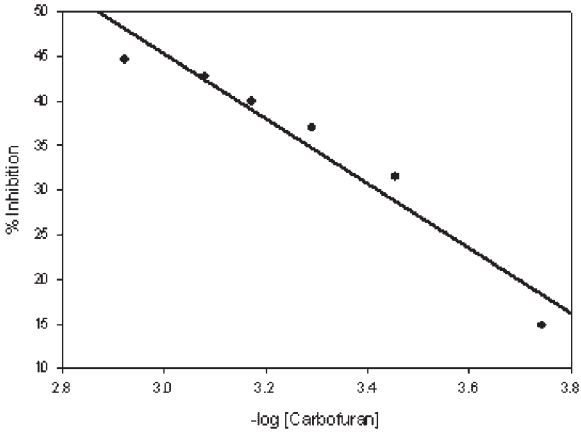

Figure 9.
Displays the inhibition plot of percentage inhibition versus –log (carbofuran) pesticide concentration as determined with the Au/MBT/POMA-PSA/AChE/ACh biosensor in 0.1 M phosphate buffer, KCl (pH 7.2) solution.

Conclusions

We have shown that the dopant called phenanthrene sulphonic acid (PSA) can be incorporated into the backbone of the monomers, *o*-methoxyaniline (OMA) and *2,5*-dimethoxyaniline (DMA). Subsequently the nanomaterials called nano-poly(*o*-methoxyaniline-phenanthrene sulphonic acid) (nanoPOMA-PSA) and nano-poly (*2,5*-dimethoxyaniline-phenanthrene sulphonic acid) (nanoPDMA-PSA) were formed. The nanoPANI-PSAs were then characterised using techniques such as scanning electron microscopy (SEM), FTIR spectroscopy, UV-Vis absorption spectroscopy, SNIFTIR spectroscopy and electrochemical techniques to elucidated the structures of the nanoPANIs and showed that polyaniline (PANI) form indeed the backbone of the nanomaterials. Both the two nanopolymers exhibited quinoid and benzoid bands typically of the polyaniline FTIR-spectra. Furthermore, the results for UV-Vis spectra shows bands and shifts indicating that phenanthrene sulphonic acid (PSA) was incorporated into the POMA and PDMA backbone respectively. Polymeric nanorod morphology for POMA-PSA and PDMA-PSA were ascertained by SEM graphs. Cyclic voltammetric characterisation of the polymer pastes showed distinctive redox couples representing various redox states assessable in the PANI polymer. Thus by applying appropriate potential the polymeric nanorods can be stabilised at required oxidation states. These results support the view that the nanoPOMA-PSA and nanoPDMA-PSA could prove promising for developing novel electrocatalysts for use in sensor devices. The nanoPOMA-PSA material was then incorporated to form the Au/MBT/POMA-PSA/AChE/ACh biosensor for pesticide analysis.

The ability of the Au/MBT/POMA-PSA/AChE/ACh biosensor wherein the enzyme acetylcholinesterase was immobilised in a conducting polymer matrix, was demonstrated. A SAM of mercaptobenzothiazole (MBT) was prepared on an Au electrode. Mercaptobenzothiazole (MBT) is different to the alkanethiols normally used, as it contains an aromatic ring that is fused with a thiazole ring, instead of long alkyl chains. It was shown that MBT could be used for pre-organisation of the Au electrode surface for drop coating of the conducting polymer. The Au/MBT/POMA-PSSA/AChE/ACh biosensor was furthermore successfully applied to the pesticide inhibition study of diazinon and carbofuran pesticides. The results of the inhibition study has showed that diazinon inhibited the enzyme AChE 91% and carbofuran by 45% in the biosensor inhibition studies performed. Furthermore, for diazinon as pesticide the theoretical detection limit was determined to be 0.14 ppb and for Carbofuran as pesticide, a detection limit of 0.06 ppb was achieved.

Acknowledgements: The authors wish to express their gratitude to the National Research Foundation (NRF), South Africa, for funding and financial support and the Department of Chemistry, University of the Western Cape for their support and funding to perform this work. Our gratitude also to the Department of Agriculture (DoA), South African Agricultural Food, Quarantine & Inspection Services (SAAFQIS) – Analytical Services South in Stellenbosch, for the supply of some pesticide standards.

[1] S.-S. Chen, T.-C. Wen, A. Gopalan, A. *Synth. Metals* **2003**, *132*, 133.
[2] L. Meiling, Y. Min, Y. Qin, Z. Youyu, X. Qingji, Y. Shouzhuo, *Electrochim. Acta* **2006**, *52*, 342.
[3] Z. A. Hu, L. J. Ren, X. J. Feng, Y. P. Wang, Y. Y. Yang, J. Shi, L. P. Mo, Z. Q. Lei, *Electrochem. Commun.* **2007**, *9*, 97.
[4] A. Morrin, O. Ngamna, A. J. Killard, S. E. Moulton, M. R. Smyth, G. G. Wallace, *Electroanal.* **2005**, *17*, 5–6, 423.
[5] L. Zhang, M. Wan, *NanoTech.* **2002**, *13*, 750.
[6] Z. Zhang, M. Wan, *Synth. Met.* **2002**, *128*, 83.
[7] Z. Zhang, Z. Wei, M. Wan, *Macromol.* **2002**, *35*, 5937.
[8] H. J. Barraza, F. Pompeo, E. A. O'Rear, D. E. Resasco, *Nano. Lett.* **2002**, *2*(8), 797.
[9] S. K. Tripathy, J. Kumar, H. S. Nalwa, "*Handbook of Polyelectrolytes and Their Applications. Polyelectrolytes, Their Characterization and Polyelectrolyte Solutions*",

Vol. 2, American Scientific Publishers, California 2002, p. 138.
[10] J. Laska, *Jnl. Molecul. Struct.* **2004**, *701*, 13.
[11] M. Del Carlo, M. Mascini, A. Pepe, G. Diletti, D. Compagnone, *Food Chem.* **2004**, *84*, 651.
[12] N. G. Karousos, S. Aouabdi, A. S. Way, A. M. Reddy, *Anal. Chim. Acta* **2002**, *469*, 189.
[13] M. Albareda-Sirvent, A. Merkoçi, S. Alegret, *Anal. Chim. Acta* **2001**, *442*, 35.
[14] A. Lima, F. Hahn, J.-M. Leger, *Russian Jnl. Electrochem.* **2004**, *40*(3), 326.
[15] S. Sotiropoulou, N. A. Chaniotakis, *Anal. Chim. Acta* **2005**, *530*, 199.
[16] M. Albareda-Sirvent, A. Merkoći, S. Alegret, *Anal. Chim. Acta* **2001**, *442*, 35.
[17] E. Wilkins, M. Carter, J. Voss, D. Ivnitski, *Electrochem. Comm.* **2000**, *2*, 786.
[18] A. R. Hopkins, R. A. Lipeles, W. H. Kao, *Thin Solid Films* **2004**, *447–448*, 474.
[19] K. R. Prasad, N. Munichandraiah, *Synth. Met.* **2001**, *123*, 459.
[20] E. I. Iwuoha, D. S. de Villaverde, N. P. Garcia, M. R. Smyth, J. M. Pingarron, *Biosens. & Bioelectron.* **1997**, *12*, 749.
[21] N. G. R. Mathebe, A. Morrin, E. I. Iwuoha, *Talanta* **2004**, *64*, 115.
[22] A. J. Bard, L. R. Faulkner, "*Electrochemical Methods: Fundamentals and Applications*", 2nd edition, Wiley, New York 2001, p. 254.
[23] Z. Zhang, M. Wan, *Synth. Met.* **2003**, *132*, 205.
[24] G. Cakmak, Z. Kucukkyavuz, S. Kucukkyavuz, *Synth. Metals* **2005**, *151*, 10.
[25] S. Pruneanu, E. Veress, I. Marian, L. Oniciu, *Jnl. Mater. Sci.* **1999**, *34*, 2733.
[26] L. Huang, T. Wen, A. Gopalan, *Synth. Met.* **2002**, *130*, 155.
[27] L. Huang, T. Wen, A. Gopalan, *Mater. Chem. & Phys.* **2002**, *77*, 726.
[28] S. R. Moraes, D. Huerta-Vilca, A. J. Motheo, *Europ. Polym. Jnl.* **2004**, *40*, 2033.
[29] S. Singh, P. R. Solanki, M. K. Pandey, B. D. Malhotra, *Anal. Chim. Acta* **2006**, *568*, 126.
[30] C. R. Raj, T. Ohsaka, *Jnl. Electroanal. Chem.* **2003**, *540*, 69.
[31] M. Mazur, P. Krysiński, *Electrochim. Acta.* **2001**, *46*, 3963.
[32] R. Brito, R. Tremont, O. Feliciano, C. R. Cabrera, *Jnl. Electroanal. Chem.* **2003**, *540*, 53.
[33] N. G. Karousos, S. Aouabdi, A. S. Way, A. M. Reddy, *Anal. Chim. Acta* **2002**, *469*, 189.
[34] C. La Rosa, F. Pariente, L. Hernández, E. Lorenzo, *Anal. Chim. Acta* **1995**, *308*, 129.

